# On the high energy pulsar population detected by Fermi

**G. A. Caliandro[1], E. C. Ferrara[2], D. Parent[3], R. W. Romani[4]**
**on behalf of the Fermi Large Area Telescope Collaboration**

## Abstract

The Large Area Telescope (LAT), Fermi's main instrument, is providing a new view of the local energetic pulsar population. In addition to identifying a pulsar origin of a large fraction of the bright unidentified Galactic EGRET sources, the LAT results provide a great opportunity to study a sizable population of high-energy pulsars.
Correlations of their physical properties, such as the trend of the luminosity versus the rotational energy loss rate, help identify global features of the gamma-ray pulsar population. Several lines of evidence, including the light curve and spectral features, suggest that gamma-ray emission from the brightest pulsars arises largely in the outer magnetosphere.

Since the launch of the Fermi satellite and during its first six months of data taking in survey mode the pulsar population discovered in the gamma-ray sky is grown as far as 46 objects. All their features and a first study of the new population are summarized in 'The First Fermi Large Area Telescope Catalog of Gamma-ray Pulsars' [1].
Fermi data were analyzed to search for pulsations using 762 contemporaneous ephemerides obtained from radio telescopes and 5 from X-ray telescopes. A group of 218 of these ephemerides come from a list of good candidate gamma-ray pulsars selected with spin-down power greater than $10^{34}$ erg $s^{-1}$. The rest of the ephemerides is a sample of 544 pulsars from nearly the entire P–Pdot plane, reducing in this way the possible bias of the LAT pulsar searches. In total the LAT detected 29 radio-selected pulsars, 5 of them are EGRET pulsars, and 8 are MSPs [2].
The LAT has also discovered 16 gamma-selected pulsars [3]. The discovery of these pulsars, as well as the determination of their timing ephemerides come directly from LAT gamma-ray data. Including Geminga, the new population counts 17 gamma-selected pulsars. A campaign to search for their radio counterpart started soon and three of them have already been found [4][5]. However, with good probability some of them are true radio-quiet gamma-ray pulsars, as in the case of CTA1 [6] and PSR 1836+5925, that were deeply searched for radio pulsations in the past.
With this large population of pulsars statistical studies on their features can be performed, that allow to better understand their physics and emission mechanisms.

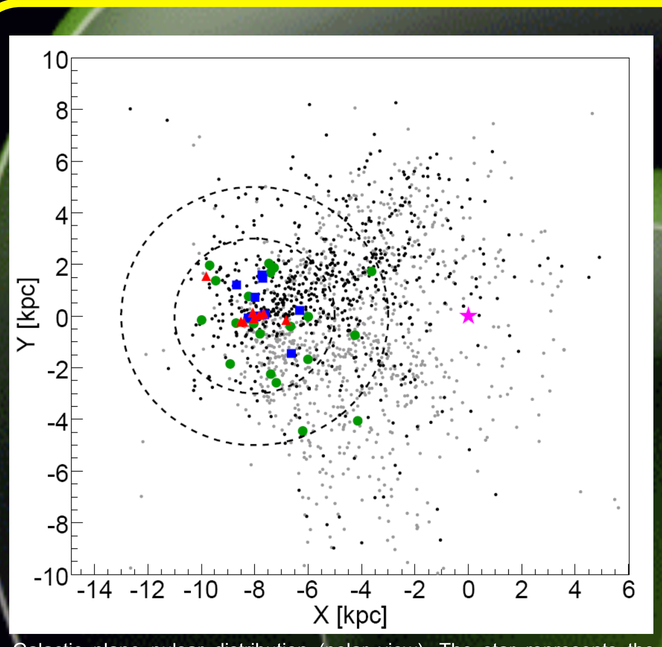


Galactic plane pulsar distribution (polar view). The star represents the Galactic center. The two circles centered at the Earth's position have radii of 3 kpc and 5 kpc. Blue squares: gamma-selected pulsars. Red triangles: millisecond gamma-ray pulsars. Green circles: all other radio loud gamma-ray pulsars. Black dots: Pulsars for which gamma-ray pulsation searches were conducted using rotational ephemerides. Gray dots: Known pulsars which were not searched for pulsations.

The pulsar distribution on the Galactic plane clearly shows that the LAT is detecting a local population of gamma-ray pulsars, most of them not farther than 3 kpc (the inner circle in the figure).
To evaluate the Galactic pulsar distribution as well as their luminosity, a good knowledge of the distances is needed. The annual trigonometric parallax methods give the most precise estimate of the distance, but unfortunately it is available only for few nearby pulsars. Among the other methods, the most commonly used estimates the pulsar distance from the radio dispersion measure (DM) coupled to an electron density distribution model, as the NE2001 [7]. When distances from different methods disagree and no one is more convincing than the other, a distance range is assumed and the luminosity is estimated for the two edge of the range, while in the Galactic distribution plot only the lower edge is drawn.
At least 19 of the 46 LAT gamma-ray pulsars are positional associated with a PWN and/or SNR, and 9 of them are associated with TeV sources. Those pulsars with both TeV and PWN associations are typically young, with ages less than 20 kyr. There are at least 3 more pulsars associated with TeV sources but not with PWNs or SNR.
Among the LAT gamma-ray pulsars, 17 were unidentified EGRET sources. This result improves the discussions about the nature of the Galactic unidentified EGRET sources, as well as the discussion on the pulsars emission models. Population synthesis studies have shown that the expected ratio of radio-loud and radio-quiet pulsars strongly depends on the assumed emission model. The total Galactic birthrate of energetic pulsars evaluated from the LAT sample is of ~1/50 yr, with gamma-selected object representing half or more. The small ratio of radio-selected to gamma-selected gamma-ray pulsars suggests that gamma-ray emission has an appreciably larger extent than the radio beams, such as expected in the outer gap (OG) [8] and slot-gap/two pole caustic (SG/TPC) models [9][10].

Gamma-ray luminosity $L_\gamma$ versus the rotational energy loss rate $\dot{E}$.

Many models for the gamma-ray emitting gap predict that the gamma-ray luminosity of the pulsars is proportional to the root square of the spin-down power ($L_\gamma \propto \dot{E}$). This imply that the gamma-ray efficiency increases with decreasing $\dot{E}$, down to ~$10^{34}$–$10^{35}$ erg $s^{-1}$ where the gap saturates at large efficiency. However the luminosity evolution of the LAT pulsars sample seems more complicated.
At high $\dot{E}$ (>$10^{36.5}$ erg $s^{-1}$) the data seems to be in rough agreement with the predicted trend. For $10^{35}<\dot{E}<10^{36.5}$ erg $s^{-1}$ $L_\gamma$ seem nearly constant, but the uncertainties in this range are very large and could hide the true luminosity evolution. In the range $10^{34}<\dot{E}<10^{35}$ erg $s^{-1}$ the gap saturation is expected to occur in both Slot Gap (~$10^{35}$ erg $s^{-1}$) and Outer Gap models (~$10^{34}$ erg $s^{-1}$) and at least for the OG model $f_\Omega$ is expect to drop well below 1. However, with the wide range of gamma-ray efficiencies in the plot it is not possible to discriminate between these model predictions. Finally for $\dot{E}<10^{34}$ erg $s^{-1}$ the sample is dominated by the MSPs and the trend seems more consistent with $\dot{E}$.

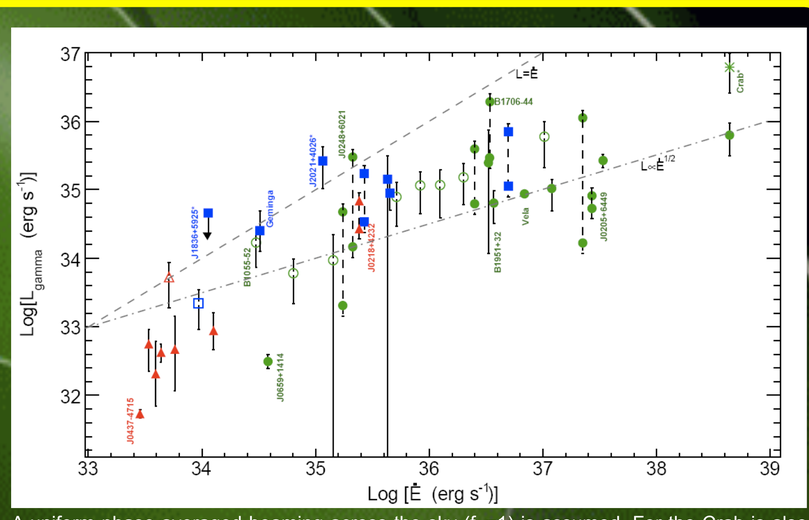


A uniform phase-averaged beaming across the sky ($f_\Omega$=1) is assumed. For the Crab is also plotted the total high energy luminosity, $L_{tot} = L_X + L_\gamma$. Empty markers refer to distances evaluated with the DM method. Two markers connected with dashed errors bars are for pulsars with an assumed range of distances . Blue squares: gamma-selected psrs. Red triangles: MSPs. Green circles: all other radio loud gamma-ray psrs.

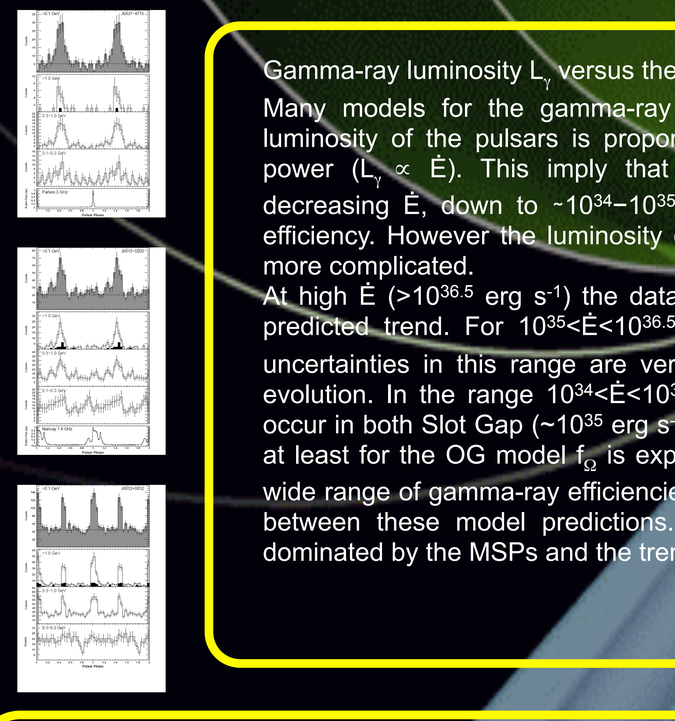


Phase difference Δ between the gamma-ray peaks, versus the phase lag δ between the main radio peak and the nearest gamma-ray peak. Pulsars without a radio detection are plotted with δ = 0. With present light curves we cannot generally measure Δ < 0.15; objects classified as single-peaked are plotted with Δ = 0. Two such objects, both MSPs, are off the plot at δ > 0.8. Blue squares: gamma-ray-selected pulsars. Red triangles: millisecond gamma-ray pulsars. Green circles: all other radio loud gamma-ray pulsars.

The pulse shape properties can help to probe the geometry and physics of the emission region. Most of the pulsars show two dominant, relatively sharp peaks, suggesting the caustics from the edge of a hollow cone. When a single peak is seen, it tends to be broader, suggesting a tangential cut through an emission cone. This picture is realized in the Outer Gap and the high altitude portion of the Slot Gap models. As well, these models predict the observed correlation of the phase lag between the radio and the first gamma-ray peak (δ) with the separation of the two gamma-ray peaks (Δ).

The spectrum energy of all the LAT gamma-ray pulsars is well fitted by a power-law with an exponential cut-off. The values of the cut-off energy ($E_c$) have a range of only about a decade, from 1 to 10 GeV, and are weakly correlated with the magnetic field at the light cylinder ($B_{LC}$).
The fact that this features are common to all the different types of pulsars strongly implies that the gamma-ray emission originates in similar locations in the magnetosphere relative to the light cylinder. Such a correlation of $E_c$ with $B_{LC}$ is actually expected in all outer magnetosphere models where the gamma-ray emission primarily comes from curvature radiation of electrons whose acceleration is balanced by radiation losses [9][11][12].
The spectral indices are distributed around ~1.5 and there is a general trend for the young pulsars to show a softer spectrum at large $\dot{E}$. This may be indicative of higher pair multiplicity, which would steepen the spectrum for the more energetic pulsars, either by steepening the spectrum of the curvature radiation-generating primary electrons [13] or by inclusion of an additional soft spectral component associated with robust pair formation [14][15].

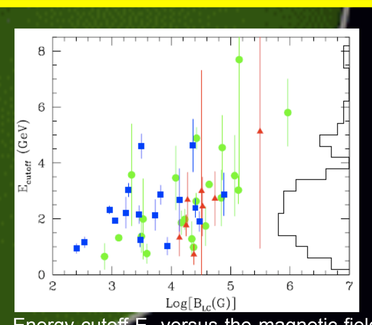


Energy cutoff $E_c$ versus the magnetic field at the light cylinder, $B_{LC}$. The histogram of $E_c$ values is along the right-hand axis.

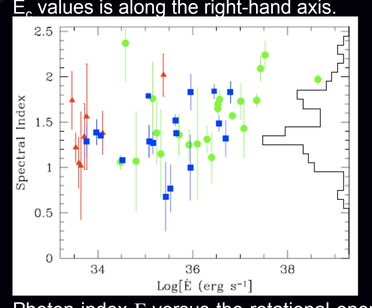


Photon index Γ versus the rotational energy loss rate, $\dot{E}$. The histogram of the Γ values is projected along the right-hand axis.

REFERENCES
[1] Abdo, A. A. et al. 2009, submitted to ApJ, arXiv0910.1608A
[2] Abdo, A. A. et al. 2009, Science, 325, 848
[3] Abdo, A. A. et al. 2009, Science, 325, 840
[4] Camino, F. et al. 2009, ApJ, 705, 1
[5] Abdo, A. A. Et al. submitted to ApJ
[6] Abdo, A. A. et al. 2008, Science, 322, 1218
[7] Cordes, J. M., & Lazio, T. J. W. 2002, arXiv:astro-ph/0207156
[8] Romani, R. W., & Yadigaroglu, I.-A. 1995, ApJ, 438, 314
[9] Muslimov, A. G. & Harding, A. K. 2004, ApJ, 606, 1143
[10] Dyks, J. & Rudak, B. 2003, ApJ, 598, 1201
[11] Zhang, L. et al. 2004, ApJ, 604, 317
[12] Hirotani, K. 2008, ApJ, 688, L25
[13] Romani, R. W. 1996, ApJ, 470, 469
[14] Takata, J., & Chang, H.-K. 2007, ApJ, 670, 677
[15] Harding, A. K. et al. 2008, ApJ, 680, 1378

AFFILIATIONS:
1: Institut de Ciencies de l'Espai (IEEC-CSIC), Campus UAB, 08193 Barcelona, Spain
2: NASA Goddard Space Flight Center, Greenbelt, MD 20771, USA
3: CNRS/IN2P3, Centre d´´ Etudes Nucl´eaires Bordeaux Gradignan, UMR 5797, Gradignan, 33175, France
4: W. W. Hansen Experimental Physics Laboratory, Kavli Institute for Particle Astrophysics and Cosmology, Department of Physics and SLAC National Accelerator Laboratory, Stanford University, Stanford, CA 94305, USA